



OPEN

Pd NPs supported on halloysite functionalized with Schiff base as an efficient catalyst for Sonogashira reaction

Mansoureh Daraie, Majid M. Heravi✉, Yalda Rangraz & Zahra Besharati

A hybrid system was designed and synthesized through reacting modified halloysite (Hal-Cl) with Schiff base (DAB-PC) and applied as catalytic support for anchoring Pd NPs to afford Pd@Hal-DAB-PC catalyst. The resultant material was well identified by various analyses including Fourier transform infrared spectroscopy (FT-IR), X-ray diffraction patterns (XRD), thermogravimetric analysis (TGA), field-emission scanning electron microscopy (FE-SEM), energy-dispersive X-ray spectroscopy (EDS), transmission electron microscopy (TEM), and inductively coupled plasma-optical emission spectrometry (ICP-OES) and revealed outstanding catalytic activity in the Sonogashira reaction in aqueous media. Also, This nanocatalyst was simply collected and recycled up to six runs with a slight drop in efficiency, indicating the durability of Pd@Hal-DAB-PC.

Nowadays, catalysts play a pivotal role in approximately 85–90% of the modern processes in the chemical industries because they can decrease the risk associated with the preparation and utilization of different chemical compounds. Despite this, homogeneous catalysts suffer from shortcomings including considerable difficulties in the separation and recycling and low chemical and thermal stability. Hence, the design and fabrication of metal nanoparticles (MNPs) based-heterogeneous catalysts are highly desirable^{1,2}.

The immobilization of the MNPs onto robust supports with large surface area preserves them from agglomeration during the manufacture of the catalyst or in a catalytic reaction and improves their efficiency and stability^{3–7}.

Recently, the organic and inorganic nanotubular materials have been widely utilized as catalytic supports due to their outstanding surface area and unique tubular morphology with an empty cavity^{8–12}.

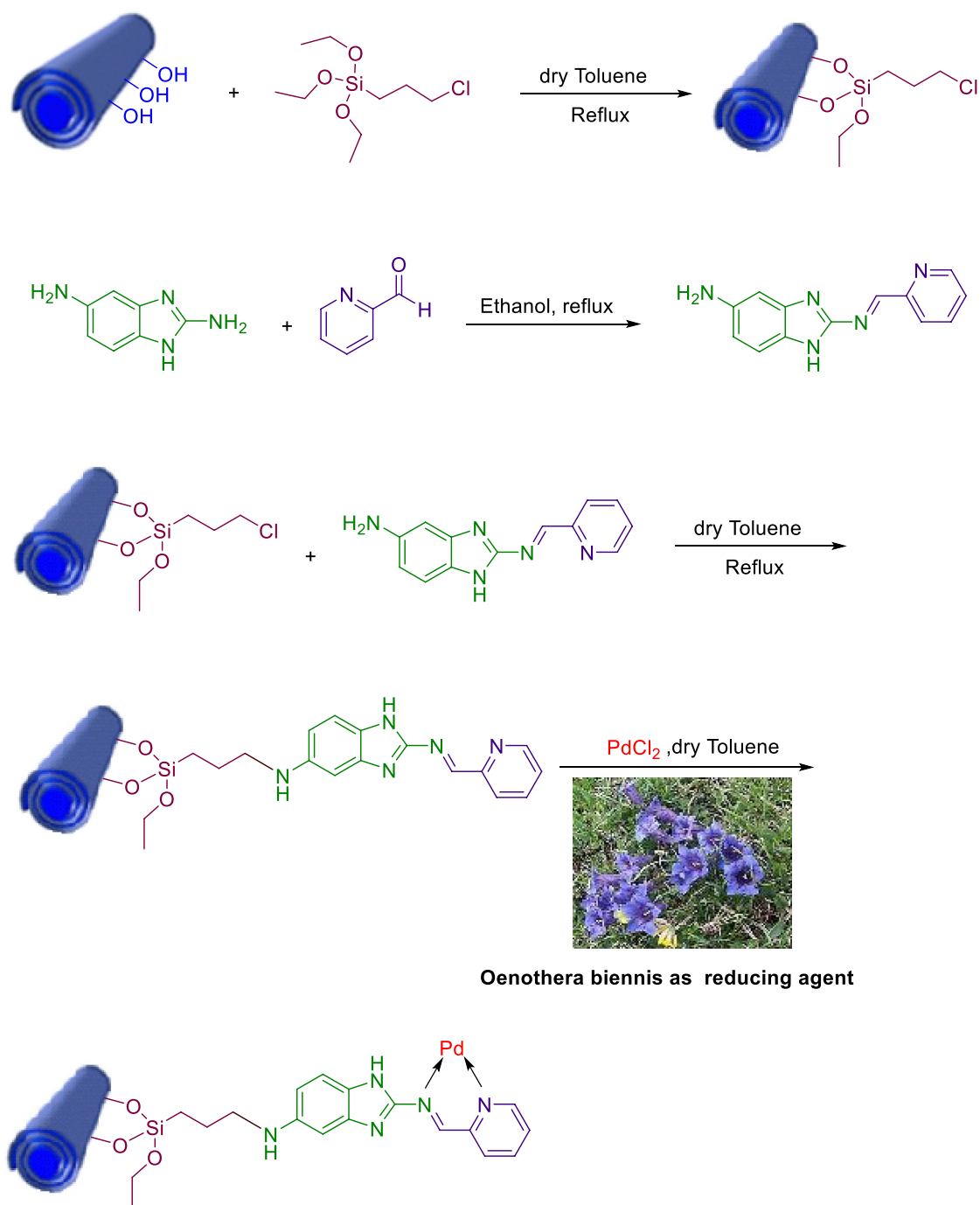
In this regard, halloysite (Hal), an octahedral layered aluminosilicate with the formula of $\text{Al}_2(\text{OH})_4\text{Si}_2\text{O}_5 \cdot n\text{H}_2\text{O}$ has gained increasing attraction in diverse scientific and industrial fields such as drug delivery, adsorbents, cleaning, and catalysis owing to high chemical and mechanical stability as well as tubular structure. Although physical and chemical features of this naturally occurring clay are similar to kaolin, some characteristics like adjustable surface chemistry and chemical composition on the inner and outer surfaces and various electrical charges make it different from classical ones^{13–15}.

Schiff bases have developed as an important research field because of structural diversity and facile preparation from the condensation of carbonyl compounds with primary amines. Moreover, metal complexes of Schiff bases display a diverse range of biological activities and also catalytic activity in different transformations^{16–19}.

Among palladium-catalyzed cross-coupling reactions, the Sonogashira cross-coupling which allows the construction of C (sp²)-C (sp) bonds by coupling aryl or vinyl halides with terminal alkynes is one of the prominent and practical synthetic methods in organic synthesis¹⁸. The resultant aryl alkynes and conjugated enynes are extensively utilized in the fabrication of polymers, pharmaceutical compounds, natural products, substituted alkynes, as well as optical materials^{21–24}.

As a part of our efforts towards developing environmentally-friendly catalytic systems for chemical transformations, such as cross-coupling reactions^{26–30}, herein, we described the fabrication of a novel heterogeneous catalyst, Pd@Hal-DAB-PC, using a multi-step modification of halloysite and stabilization of Pd NPs (Scheme 1) and its utilization in the Sonogashira reaction.

Department of Chemistry, School of Science, Alzahra University, Vanak, Tehran, Iran. ✉email: mmh1331@yahoo.com

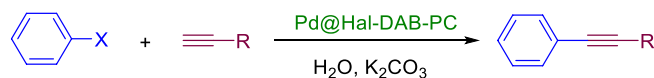


Scheme 1. The representation of the fabrication of Pd@ Hal-DAB-PC.

Experimental

Materials and instruments. All the materials utilized for the fabrication of the catalyst and doing Sonogashira reactions, such as Hal, CPTES, 1*H*-benzimidazole-2,5-diamine (DAB), pyridine-2-carbaldehyde (PC), triethylamine, palladium chloride, aryl halides, propargyl alcohol, phenylacetylene, NaOH, K₂CO₃, toluene, ethanol, and methanol were obtained from Sigma-Aldrich and applied as supplied.

The successful synthesis of Pd@Hal-DAB-PC was affirmed using different techniques involving FT-IR, XRD, TGA, FE-SEM, EDX, ICP, and TEM.



Scheme 2. Sonogashira reaction catalyzed by Pd@Hal-DAB-PC.

In catalytic characterizations, FT-IR spectra were recorded by using PERKIN-ELMER-Spectrum 65 instrument. SEM analysis was carried out over a FESEM-TESCAN MIRA3 microscope with attached EDX (TSCAN). XRD was recorded using Cu K α radiation (wavelength of 1.78897 Angstrom, 40 keV and 40 Ma). Transmission electron microscope (TEM) images were recorded with CM30300 Kv field emission transmission electron microscope. To perform ICP analysis, an ICP analyzer (Vista-pro, Varian) was employed. A Mettler Toledo TGA instrument was employed for accomplishing TGA, using nitrogen atmosphere. NMR spectra of the organic compounds were measured with a BRUKER spectrometer.

Fabrication of Pd@Hal-DAB-PC. *Fabrication of Hal-Cl (Hal modification with (3-chloropropyl)triethoxysilane (CPTES)).* First, 1.5 g of Hal was ultrasonically spread in 40 ml of dry toluene for 30 min. In the following, 1.5 g of CPTES was dropwise injected into the above suspension and next refluxed under flowing N₂ for 24 h. Finally, the resulting mixture was filtered and repeatedly rinsed with toluene. After drying in an oven at 80 °C for 24 h, Hal was decorated with CPTES.

Synthesis of the Schiff base ligand (DAB-PC). 0.108 g of Pyridine-2-carbaldehyde (1.0 mmol) was reacted with 0.147 g of benzimidazole-2,5-diamine (1.0 mmol) in EtOH for 4 h at reflux temperature. The resulting pale-yellow solid was separated by filtration. After drying, (2-((pyridine-2-ylmethylene)amino)-1H-benzo[d]imidazole 5-amine) was provided as a pale yellow powder³¹.

Incorporation of Schiff base: synthesis of Hal-DAB-PC. Initially, 1.5 g of Hal-Cl was spread in the dry toluene by sonication. In the following, 1.5 g of Schiff base was added to the mentioned suspension in the attendance of 2 ml of triethylamine as a catalyst and subsequently, heated at 110 °C for 1 day. The resultant solid was collected after completing the reaction, rinsed with dry toluene several times, and next dried at 100 °C for 24 h.

Preparations of Oenothera biennis extract. Firstly, 2 g of Oenothera biennis which were collected from Kurdistan, Iran, ground in a porcelain mortar. After that, the obtained powder was thoroughly mixed with 100 ml of deionized water and heated for 1 h at 80 °C. The resulting solid was isolated using facile filtration after cooling the mixture, and the extract was achieved.

Immobilization of Pd nanoparticles on Hal-DAB-PC by using Oenothera biennis extract as a reducing agent. For the immobilization of Pd NPs, 1.2 g of Hal-DAB-PC was added to 15 ml of dry toluene that containing 0.02 g palladium chloride was, followed by stirring for 12 h at ambient temperature. In the next step, 10 ml of Oenothera biennis extract was added and the resultant mixture was allowed to stir for another 5 h. The final product was isolated, rinsed with MeOH (three times), and then dried in an oven at 60 °C for 24 h to provide Pd@ Hal-DAB-PC (Scheme 1).

General method for Sonogashira reaction. To a mixture of aryl halide (1 mmol) and terminal alkyne (1.2 mmol) in H₂O as the solvent, Pd@Hal-DAB-PC (10 mol%) and K₂CO₃ (3 mmol) were added and the resulting mixture was heated at 100 °C for the desired time (Scheme 2). The proceeding of the reaction was followed by TLC. After finishing the reaction, the Pd@Hal-DAB-PC was isolated, washing done with EtOH, dried, and then reused for the next run under similar conditions. The organic layer was extracted via diethyl ether and purified using column chromatography [*n*-hexane/ethyl acetate (4:1)] to gain the respective product.

Result and discussion

Characterization of catalyst. The FT-IR spectra of Hal, Hal-DAB-PC, and Pd@Hal-DAB-PC are illustrated in Fig. 1. In the FT-IR spectrum of Hal, the prominent absorption peaks at 536, 1651, and 3627–3700 are ascribed to the stretching vibrations of Al–O–Si, Si–O, and inner -OH groups, respectively³². The emergence of a new absorption peak at 1625 cm⁻¹ corresponding to stretching vibration of C=N in the FT-IR spectrum of Hal-DAB-PC affirms the successful synthesis of Schiff base. There is not an obvious change in the spectrum of Pd@Hal-DAB-PC, suggesting that the immobilization of Pd does not influence the distinctive peaks of Hal-DAB-PC.

The morphology, as well as the chemical composition of Pd@Hal-DAB-PC, were surveyed by FE-SEM and EDS analyses (Figs. 2, 3). The SEM image of the catalyst exhibits that the tubular morphology of Hal remained unchanged after modification with Schiff base and incorporation of Pd NPs. Also, the EDX spectrum of the Pd@Hal-DAB-PC demonstrates the presence of Al, Si, and O elements which are ascribed to the Hal structure. Apart

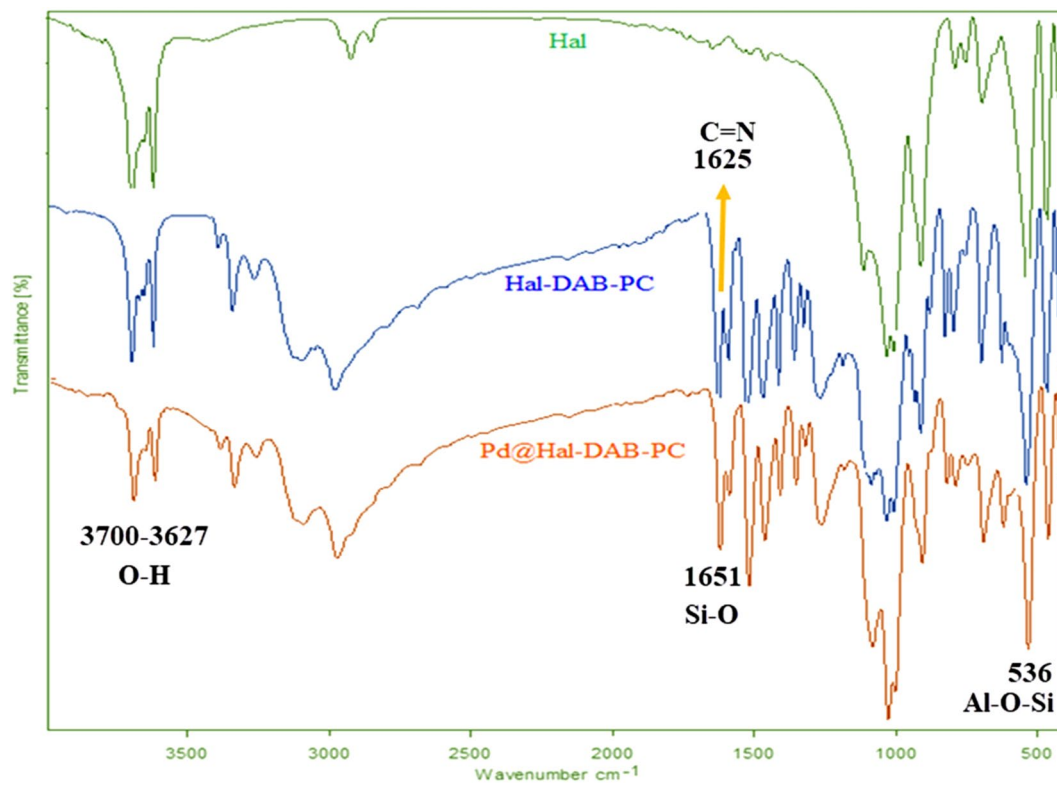


Figure 1. The FTIR spectrums of Hal, Hal-DAB-PC, and Pd@Hal-DAB-PC.

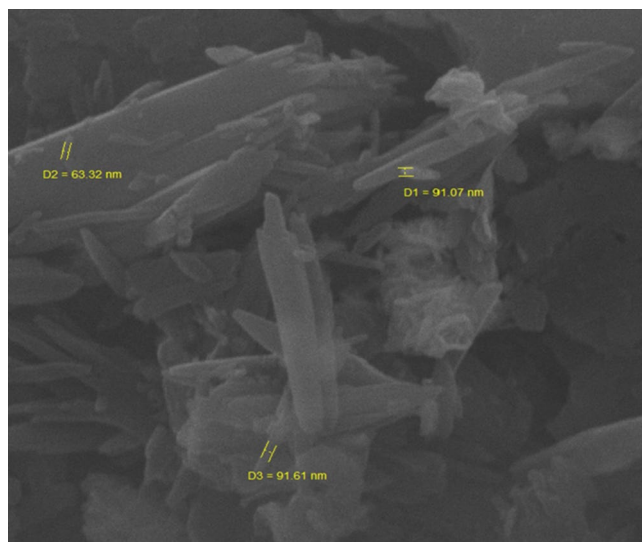


Figure 2. SEM image of Pd@Hal-DAB-PC.

from these elements, the observation of the peaks of C, N, and Pd authenticates the attendance of Schiff base as well as Pd NPs in the final structure of Pd@Hal-DAB-PC.

Also, the EDX spectrum of the Pd@Hal-DAB-PC demonstrates the presence of Al, Si, and O elements which are ascribed to the Hal structure. Apart from these elements, the observation of the peaks of C, N, and Pd authenticates the attendance of Schiff base as well as Pd NPs in the final structure of Pd@Hal-DAB-PC.

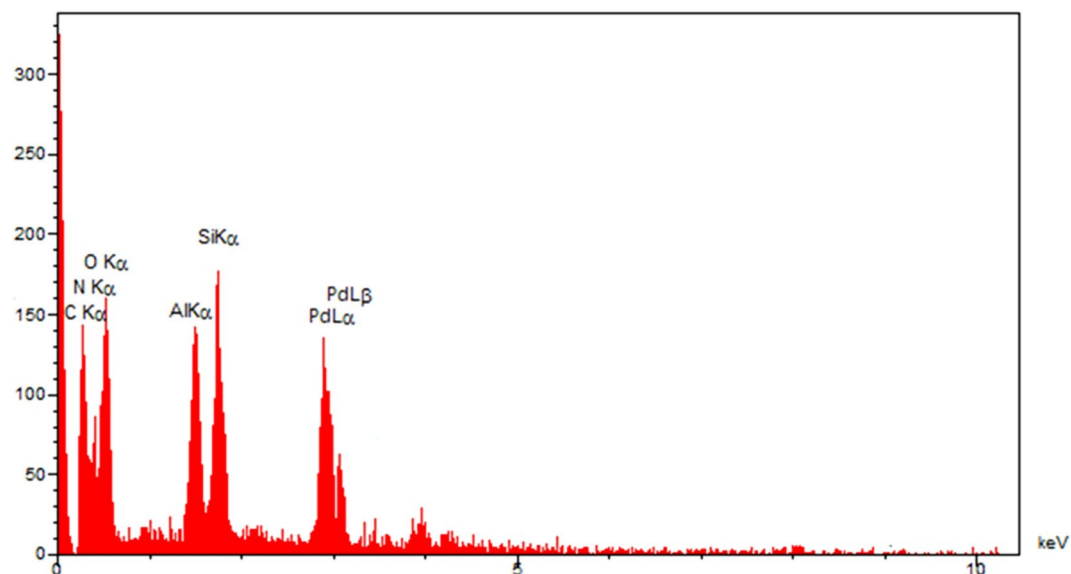


Figure 3. EDX spectrum of Pd@Hal-DAB-PC.

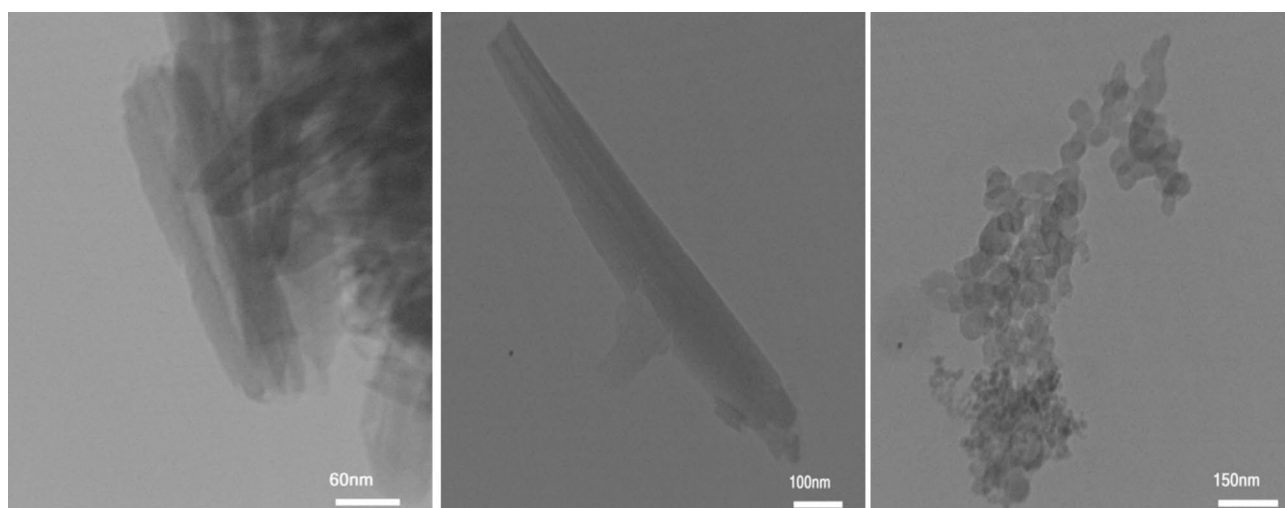


Figure 4. TEM images of Pd@Hal-DAB-PC.

The surface structure and morphology of the Pd@Hal-DAB-PC nanocatalyst were further studied using TEM. The TEM images of the Pd@Hal-DAB-PC displayed the tubular morphology of Hal. Besides, Pd NPs can be seen on the surface of the support, confirming immobilization of Pd NPs (Fig. 4).

In the following, the thermostability of the catalyst and the percentage of the organic groups linked to the surface of the Hal were examined using TGA. The thermograph of the Pd@Hal-DAB-PC depicts three decomposition steps (Fig. 5). The initial weight reduction (about 10–12%) at low temperatures (70–120 °C) can be related to the removal of the adsorbed water and surface hydroxyl groups. A higher weight loss (10–20%) in the region 330–410 °C corresponds to the decomposition of the Schiff base segment and the chloropropyl groups grafted to the Hal. The next minimal weight loss is due to the elimination of chemisorbed water. The observed total weight reduction is 33.97 until 700 °C. These results show good thermal stability of Pd@Hal-DAB-PC.

To obtain information about the crystalline nature and phase composition of the Pd@Hal-DAB-PC, X-ray powder diffraction (XRD) analysis was accomplished. The XRD curve of the Pd@Hal-DAB-PC (Fig. 6) reveals the distinctive peaks at $2\theta = 8^\circ, 12^\circ, 22.6^\circ, 28.2^\circ, 31.5^\circ, 57^\circ,$ and 68° which are in good record with the XRD pattern of Hal (JCPDS card no. 29-1487)^{33,34}. This result confirms that the tubular structure of Hal does not destroy during the functionalization and stabilization of Pd. Also, the diffraction peaks of Pd NPs were not observed in the sample, affirming the high dispersion of Pd NPs as well as their low loading on the support³⁵. This result was confirmed by ICP analysis and the loading of Pd was found to be 0.85 wt%.

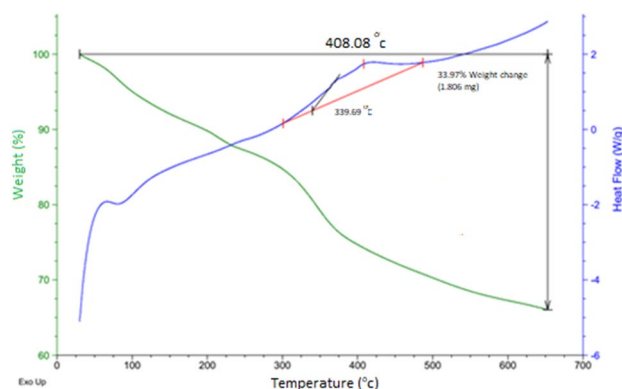


Figure 5. The TGA curve of Pd@Hal-DAB-PC.

Catalytic activity. After the successful synthesis and identification of Pd@Hal-DAB-PC, its catalytic behavior was evaluated in the Sonogashira coupling reaction. For this purpose, the coupling of iodobenzene with phenylacetylene was chosen as a probe reaction and the efficient parameters on this reaction like catalyst amount, temperature, and type of solvent and base were optimized to achieve the highest product yield. The results were summarized in Table 1. K_2CO_3 as a base in the presence of H_2O as a green solvent and 10 mol% of Pd@Hal-DAB-PC at 80 °C was found to be the best reaction conditions.

In the next step, the wide utilization of Pd@Hal-DAB-PC was further examined (Table 2). A broad set of aryl iodides involving electron-withdrawing, electron-donating, and sterically hindered groups effectively reacted with terminal alkynes to furnish the respective products in high yields. All compounds are known and their

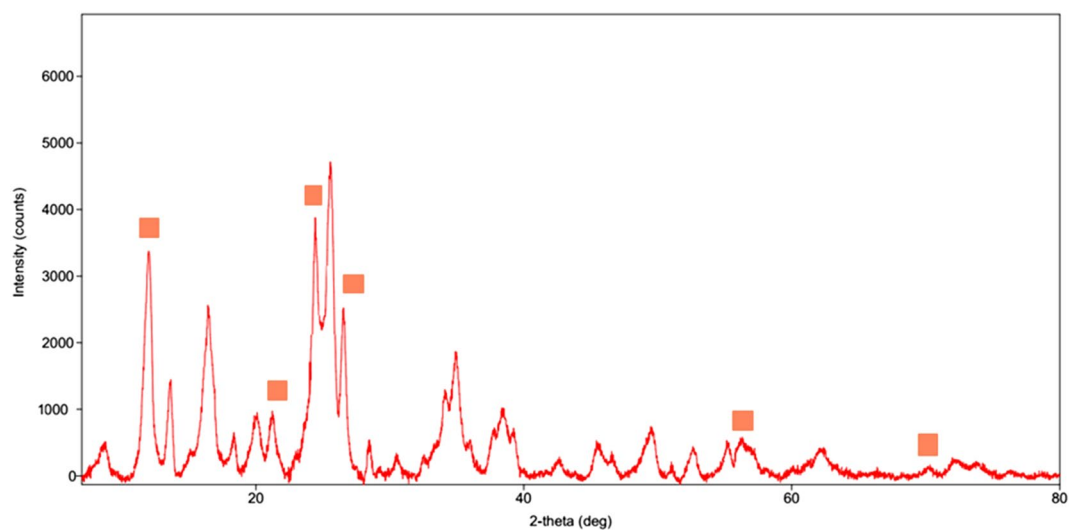


Figure 6. The XRD curve of Pd@Hal-DAB-PC.

physical data were compared and validated with those of authentic samples. Some selected spectral data are presented in supporting information (Figures S1–S10).

Interestingly, good yields of products are also provided in the coupling of less-reactive (more challenging) aryl chloride with various terminal alkynes.

Entry	Reaction condition	Catalyst (mol%)	Base	Time (h)	Yield (%)
1	H ₂ O/r.t	10	K ₂ CO ₃	3	90
2	H ₂ O/50 °C	10	K ₂ CO ₃	2.5	92
3	H ₂ O/80 °C	10	K ₂ CO ₃	2	97
4	H ₂ O/reflux	10	K ₂ CO ₃	2	95
5	EtOH, r.t	10	K ₂ CO ₃	3	82
6	EtOH, reflux	10	K ₂ CO ₃	2.5	88
7	CH ₃ CN, reflux	10	K ₂ CO ₃	3	85
8	CHCl ₃ , reflux	10	K ₂ CO ₃	3.2	80
9	Toluene, 80 °C	10	K ₂ CO ₃	2.8	79
10	H ₂ O/80 °C	15	K ₂ CO ₃	2	96
11	H ₂ O/80 °C	5	K ₂ CO ₃	2.5	82
12	H ₂ O/80 °C	10	NaOH	2.5	84

Table 1. Optimization for the coupling of aryl iodide and phenyl acetylene^a. ^aReaction conditions: iodobenzene (1 mmol), phenylacetylene (1.2 mmol), base (3 mmol), and solvent (5 ml).

Mechanism. A reasonable mechanistic pathway was suggested as depicted in Scheme 3. Accordingly, initial oxidative addition of [Pd(0)L₂] to the aryl or vinyl halide takes place which is followed by reversible coordination of the alkyne, creating an alkyne-Pd(II) complex. Then, in the presence of a base, it was deprotonated with concurrent coordination of the acetylene ligand to the metal. Next, upon reductive elimination, the [Pd(II) R¹(C[tbond]CR²)L₂] complex, releases the cross-coupled product along with regeneration of the catalyst species, [Pd(0)L₂].

Reusability of Pd@Hal-DAB-PC. The stability/reusability of a catalyst is a critical factor from the economic and industrial points of view. In this context, the stability of Pd@Hal-DAB-PC was inspected in the model reaction under the optimal conditions (Fig. 7). After completion of the reaction in each run, the catalyst was collected via centrifugation, washed with ethanol, and then reused in the next cycle. The recycling experiments show that Pd@Hal-DAB-PC is highly resistant with a slight decrease in its catalytic efficiency during six runs.

To examine any effect on the catalyst morphology during the recyclization process, after six reaction runs, the recycled catalyst was submitted to the SEM analysis, (Fig. 8). As illustrated in Fig. 8, the SEM image of the recycled catalyst was compared with the freshly used catalyst and was found to be similar.

Conclusions

In summary, we reported the fabrication of Pd@Hal-DAB-PC as a new hybrid catalyst by functionalizing Cl-Hal with Schiff base and the next stabilization of Pd NPs. The obtained catalyst was capable to successfully catalyze the Sonogashira cross-coupling reactions in aqueous media under ligand- and Cu-free reaction conditions. Furthermore, Pd@Hal-DAB-PC was stable and could be reused for six runs while its efficiency was largely maintained.

Data availability

The raw/processed data that supports the findings of this study are available from the corresponding author upon reasonable request.

Received: 9 December 2020; Accepted: 1 March 2021

Published online: 18 March 2021

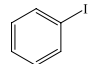
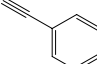

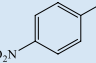
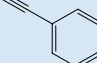
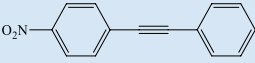
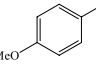
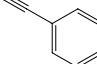
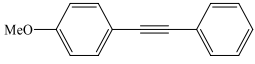
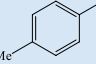
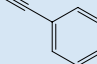
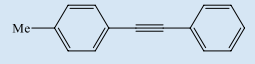
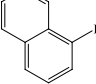
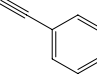
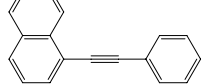
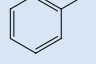
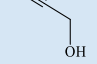
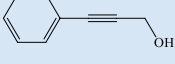
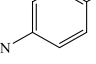
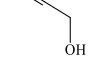
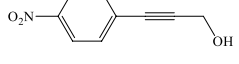
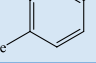
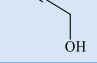
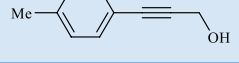
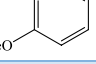
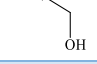
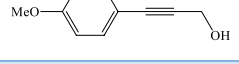
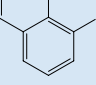
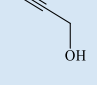
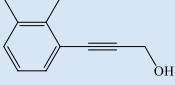
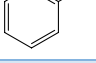
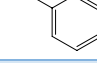

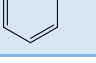
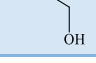
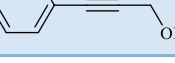
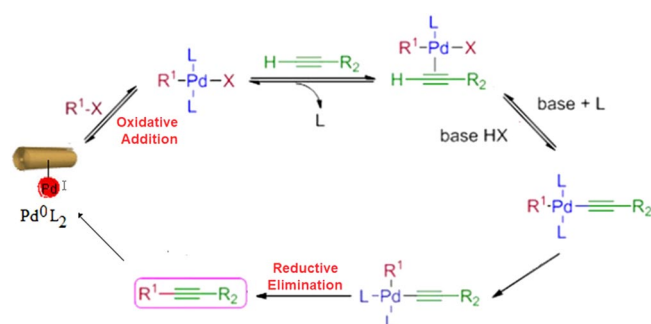
Entry	Aryl halide	Terminal alkyne	Product	Time (h)	Yield ^b (%)
1				2	97
2				2.2	94
3				2.5	95
4				2	95
5				3.8	90
6				2.5	90
7				2	92
8				3.5	89
9				3	90
10				4	89
11				4	85
12				4.5	85

Table 2. Pd@Hal-DAB-PC catalyzed Sonogashira reaction of various halides with terminal alkynes^a. ^aReaction condition: aryl halide (1.0 mmol), terminal alkyne (1.2 mmol), Pd@Hal-DAB-PC (10 mol%) and K₂CO₃ (3.0 mmol) in H₂O at 80 °C.



Scheme 3. Plausible reaction mechanism.

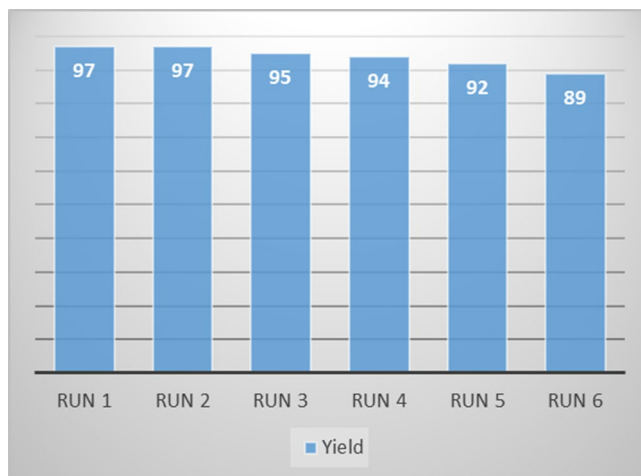


Figure 7. Reusability of Pd@Hal-DAB-PC.

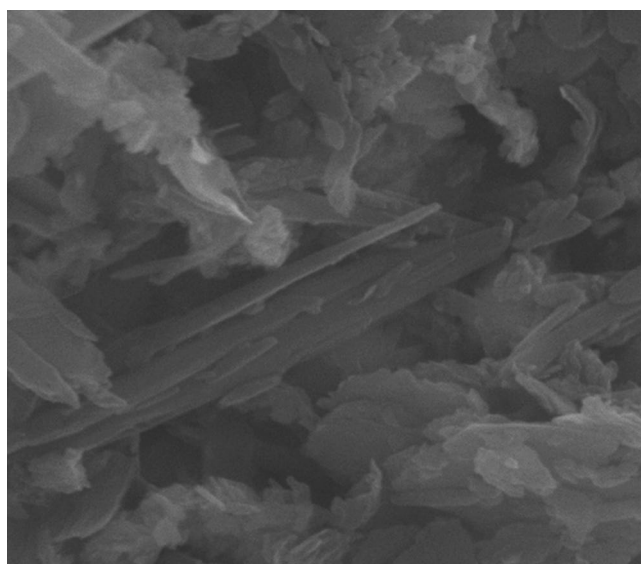


Figure 8. SEM image of the recycled catalyst after six reaction runs.

References

1. Massaro, M. *et al.* Halloysite nanotubes as support for metal-based catalysts. *J. Mater. Chem. A*, **5**, 13276–13293. <https://doi.org/10.1039/C7TA02996A> (2017).
2. Liu, J. Catalysis by supported single metal atoms. *ACS Catal.* **7**, 34–59. <https://doi.org/10.1021/acscatal.6b01534> (2017).
3. Pavia, C. *et al.* Palladium supported on cross-linked imidazolium network on silica as highly sustainable catalysts for the Suzuki reaction under flow conditions. *Adv. Synth. Catal.* **355**, 2007–2018. <https://doi.org/10.1002/adsc.201300215> (2013).
4. Petrucci, C. *et al.* *ACS Sustain. Chem. Eng.* **2**, 2813–2819 (2014).
5. Fihri, A., Bouhrara, M., Nekoueshahraki, B., Basset, J.-M. & Polshettiwar, V. Nanocatalysts for Suzuki cross-coupling reactions. *Chem. Soc. Rev.* **40**, 5181–5203. <https://doi.org/10.1039/C1CS15079K> (2011).
6. Cui, X. *et al.* Facile growth of ultra-small Pd nanoparticles on zeolite-templated mesocellular graphene foam for enhanced alcohol electrooxidation. *Nano Res.* **12**, 351–356 (2019).
7. Wu, D., Cao, M. & Cao, R. Replacing PVP by macrocycle cucurbit [6] uril to cap sub-5 nm Pd nanocubes as highly active and durable catalyst for ethanol electrooxidation. *Nano Res.* **12**, 2628–2633 (2019).
8. Liu, X. *et al.* Precise localization of metal nanoparticles in dendrimer nanosnakes or inner periphery and consequences in catalysis. *Nat. Commun.* **7**, 1–8 (2016).
9. Salvo, A. M. P., La Parola, V., Liotta, L. F., Giacalone, F. & Gruttadauria, M. Highly loaded multi-walled carbon nanotubes non-covalently modified with a bis-imidazolium salt and their use as catalyst supports. *ChemPlusChem* **81**, 471. <https://doi.org/10.1002/cplu.201600023> (2016).
10. Giacalone, F. *et al.* Supported C₆₀-IL-Pd NPs as extremely active nanocatalysts for C-C cross-coupling reactions. *J. Mater. Chem. A*, **4**, 17193–17206. <https://doi.org/10.1039/C6TA07599A> (2016).
11. Campisciano, V., LaParola, V., Liotta, L. F., Giacalone, F. & Gruttadauria, M. Fullerene-Ionic-liquid conjugates: A new class of hybrid materials with unprecedented properties. *Chem. Eur. J.* **21**, 3327–3334. <https://doi.org/10.1002/chem.201406067> (2015).

12. Tan, D. *et al.* Loading and in vitro release of ibuprofen in tubular halloysite. *Appl. Clay Sci.* **96**, 50–55. <https://doi.org/10.1016/j.clay.2014.01.018> (2014).
13. Massaro, M. *et al.* Palladium nanoparticles immobilized on halloysite nanotubes covered by a multilayer network for catalytic applications. *New J. Chem.* **42**, 13938–13947. <https://doi.org/10.1039/C8NJ02932F> (2018).
14. Abdullayev, E. & Lvov, Y. Halloysite clay nanotubes as a ceramic “skeleton” for functional biopolymer composites with sustained drug release. *J. Mater. Chem. B*, **1**, 28942903. <https://doi.org/10.1039/C3TB20059K> (2013).
15. Das, T. K. *et al.* Mussel inspired green synthesis of silver nanoparticles-decorated halloysite nanotube using dopamine: Characterization and evaluation of its catalytic activity. *Appl. Nanosci.* **8**, 173–186 (2018).
16. Molano, W. A., Cárdenas, J. C., Sierra, C. A., Carriazo, J. G. & Ochoa-Puentes, C. Pd/halloysite as a novel, efficient and reusable heterogeneous nanocatalyst for the synthesis of p-phenylenevinylene oligomers. *Chem. Sel.* **3**, 4430–4438. <https://doi.org/10.1002/slct.201800344> (2018).
17. Al Zoubi, W. & Al Mohanna, N. Membrane sensors based on Schiff bases as chelating ionophores. *Spectrochim. Acta A Mol. Biomol. Spect.* **132**, 854–870. <https://doi.org/10.1016/j.saa.2014.04.176> (2014).
18. Al Zoubi, W., Kandil, F. & Chebani, M. K. Solvent extraction of chromium and copper using Schiff base derived from terephthalaldehyde and 5-amino-2-methoxy-phenol. *Arab. J. Chem.* **9**, 526–531. <https://doi.org/10.1016/j.arabjc.2011.06.023> (2016).
19. Al Zoubi, W., Kandil, F., Chebani, K. & Zoubi, W. Active transport of metal ions by using Schiff bases. *Phys. Sci. Res. Int.* **2**, 12–23 (2014).
20. Kandil, F., Al Zoubi, W. & Chebani, M. K. The synthesis and characterization of new Schiff bases and investigating them in solvent extraction of chromium and copper. *Sep. Sci. Technol.* **47**, 1754–1761. <https://doi.org/10.1080/01496395.2012.660554> (2012).
21. Chinchilla, R. & Nájera, C. Recent advances in Sonogashira reactions. *Chem. Soc. Rev.* **40**, 5084–5121. <https://doi.org/10.1039/C1CS15071E> (2011).
22. Doucet, H. & Hierso, J. C. Palladium-based catalytic systems for the synthesis of conjugated enynes by Sonogashira reactions and related alkyneulations. *Angew. Chem. Int. Ed.* **46**, 834–871. <https://doi.org/10.1002/anie.200602761> (2007).
23. Cosford, N. D. *et al.* 3-[(2-Methyl-1, 3-thiazol-4-yl) ethynyl]-pyridine: A potent and highly selective metabotropic glutamate subtype 5 receptor antagonist with anxiolytic activity. *J. Med. Chem.* **46**, 204–206. <https://doi.org/10.1021/jm025570j> (2003).
24. Chinchilla, R. & Nájera, C. The Sonogashira reaction: A booming methodology in synthetic organic chemistry. *Chem. Rev.* **107**, 874–922. <https://doi.org/10.1021/cr050992x> (2007).
25. Balsukuri, N., Das, S. & Gupta, I. Carbazole-corrole and carbazole-prophyrin dyads: Synthesis, fluorescence and electrochemical studies. *New J. Chem.* **39**, 482–491. <https://doi.org/10.1039/C4NJ01086H> (2015).
26. Sadjadi, S., Lazzara, G., Malmir, M. & Heravi, M. M. Pd nanoparticles immobilized on the poly-dopamine decorated halloysite nanotubes hybridized with N-doped porous carbon monolayer: A versatile catalyst for promoting Pd catalyzed reactions. *J. Catal.* **366**, 245–257. <https://doi.org/10.1016/j.jcat.2018.08.013> (2018).
27. Sadjadi, S., Heravi, M. M. & Malmir, M. Pd@HNTs-CDNS-g-C₃N₄: A novel heterogeneous catalyst for promoting ligand and copper-free Sonogashira and Heck coupling reactions, benefits from halloysite and cyclodextrin chemistry and g-C₃N₄ contribution to suppress Pd leaching. *Carbohydr. Polym.* **186**, 25–34. <https://doi.org/10.1016/j.carbpol.2018.01.023> (2018).
28. Sadjadi, S., Malmir, M., Heravi, M. M. & Kahangi, F. G. Biocompatible starch-halloysite hybrid: An efficient support for immobilizing Pd species and developing a heterogeneous catalyst for ligand and copper free coupling reactions. *Int. J. Biol. Macromol.* **118**, 1903–1911. <https://doi.org/10.1016/j.ijbiomac.2018.07.053> (2018).
29. Sadjadi, S., Heravi, M. M. & Kazemi, S. S. Ionic liquid decorated chitosan hybridized with clay: A novel support for immobilizing Pd nanoparticles. *Carbohydr. Polym.* **200**, 183–190. <https://doi.org/10.1016/j.carbpol.2018.07.093> (2018).
30. Daraie, M., Heravi, M. M. & Kazemi, S. S. Pd@GO/Fe₃O₄/PAA/DCA: A novel magnetic heterogeneous catalyst for promoting the Sonogashira cross-coupling reaction. *J. Coord. Chem.* **72**, 2279–2293. <https://doi.org/10.1080/00958972.2019.1640360> (2019).
31. Qazi, S. U. *et al.* Semicarbazone derivatives as urease inhibitors: Synthesis, biological evaluation, molecular docking studies and in-silico ADME evaluation. *Bioorg. Chem.* **79**, 19–26. <https://doi.org/10.1016/j.bioorg.2018.03.029> (2018).
32. Sadjadi, S., Hosseinejad, T., Malmir, M. & Heravi, M. M. Cu@furfural imine-decorated halloysite as an efficient heterogeneous catalyst for promoting ultrasonic-assisted A³ and KA² coupling reactions: A combination of experimental and computational study. *New J. Chem.* **41**, 13935–13951. <https://doi.org/10.1039/C7NJ02272G> (2017).
33. Yuan, P., Tan, D. & Annabi-Bergaya, F. Properties and applications of halloysite nanotubes: Recent research advances and future prospects. *Appl. Clay Sci.* **112**, 75–93. <https://doi.org/10.1016/j.clay.2015.05.001> (2015).
34. Hao, D. *et al.* Synthesis of monodisperse palladium nanocubes and their catalytic activity for methanol electrooxidation. *Chin. Phys. B*, **19**, 106104–106110 (2010).
35. Sadjadi, S., Heravi, M. M., Raja, M. & Kahangi, F. G. Palladium nanoparticles immobilized on sepiolite-cyclodextrin nanosponge hybrid: Efficient heterogeneous catalyst for ligand-and copper-free C–C coupling reactions. *Appl. Organomet. Chem.* **32**, 4508. <https://doi.org/10.1002/aoc.4508> (2018).

Acknowledgements

M. Daraie and M. M. Heravi are grateful to Iran National Science Foundation (INSF) for financial support provided by the post-doctoral project (99006750). We also appreciate Alzahra University Research Council for their help and supports.

Author contributions

M.D. and M.M.H. designed the experiments, M.D. performed the experiments, M.M.H. contributed materials/analysis tools, M.D. and Y.R. wrote the paper and Z.B. prepared figures. All authors reviewed the manuscript.

Competing interests

The authors declare no competing interests.

Additional information

Supplementary Information The online version contains supplementary material available at <https://doi.org/10.1038/s41598-021-85821-2>.

Correspondence and requests for materials should be addressed to M.M.H.

Reprints and permissions information is available at www.nature.com/reprints.

Publisher's note Springer Nature remains neutral with regard to jurisdictional claims in published maps and institutional affiliations.



Open Access This article is licensed under a Creative Commons Attribution 4.0 International License, which permits use, sharing, adaptation, distribution and reproduction in any medium or format, as long as you give appropriate credit to the original author(s) and the source, provide a link to the Creative Commons licence, and indicate if changes were made. The images or other third party material in this article are included in the article's Creative Commons licence, unless indicated otherwise in a credit line to the material. If material is not included in the article's Creative Commons licence and your intended use is not permitted by statutory regulation or exceeds the permitted use, you will need to obtain permission directly from the copyright holder. To view a copy of this licence, visit <http://creativecommons.org/licenses/by/4.0/>.

© The Author(s) 2021